PHYSICAL REVIEW LETTERS

Electric Manipulation of Spin Relaxation Using the Spin Hall Effect

K. Ando,[1,*] S. Takahashi,[2,3] K. Harii,[1] K. Sasage,[1] J. Ieda,[2,3] S. Maekawa,[2,3] and E. Saitoh[1,4]

[1]*Department of Applied Physics and Physico-Informatics, Keio University, Yokohama 223-8522, Japan*
[2]*Institute for Materials Research, Tohoku University, Sendai 980-8577, Japan*
[3]*CREST, Japan Science and Technology Agency, Kawaguchi, Saitama 332-0012, Japan*
[4]*PRESTO, Japan Science and Technology Agency, Kawaguchi, Saitama 332-0012, Japan*

Using the spin Hall effect, magnetization relaxation in a $Ni_{81}Fe_{19}$/Pt film is manipulated electrically. An electric current applied to the Pt layer exerts spin torque on the entire magnetization of the $Ni_{81}Fe_{19}$ layer via the macroscopic spin transfer induced by the spin Hall effect and modulates the magnetization relaxation in the $Ni_{81}Fe_{19}$ layer. This method allows us to tune the magnetization dynamics regardless of the film size without applying electric currents directly to the magnetic layer.

Since magnetization relaxation governs the spin coherence and the magnetic response of a magnet [1], controlling it is an earnest desire in the field of spintronics [2,3] and spin-based quantum-information technology [4]. However, once material species, temperature, and pressure are selected, this relaxation is considered to be difficult to control.

A method for controlling the magnetization dynamic is the utilization of spin torque [5]. In a giant magnetoresistance or a tunnel magnetoresistance (TMR) junction, an electric current through the junction exerts spin torque on the ferromagnetic layer and modulates the magnetization relaxation. This modulation is responsible for the current-induced magnetization reversal [6], but it was believed to be usable only in a very small area of a sample since the current should be applied through the junction; in fact, experiments are limited in nanopillar devices [6–9]. Furthermore, this electric current in the small area turned out to be harmful to TMR junctions [10]. In this Letter, we show that the magnetization-precession relaxation is manipulated electrically using the spin Hall effect (SHE) regardless of the film size without nanoprocessing. This method enables electric tuning of spin dynamics without applying electric currents directly to the magnetic layer.

Relaxation time τ of the magnetization precession is measured by monitoring the width of a ferromagnetic resonance (FMR) spectrum [11]. Figure 1(b) is an example of a FMR spectrum for a ferromagnetic $Ni_{81}Fe_{19}$ plain film. In this spectrum, spectral width W, namely, the distance between the peak and the dip, equals $1/(\tau\gamma)$, where γ represents the gyromagnetic ratio.

Recently, this spectral width was found to be enhanced by attaching a metal with strong spin-orbit (SO) interaction, such as Pt [12–14]. This enhancement is attributed to the emission of a spin current, the flow of the electron's spins, from the magnetization-precession motion. Since a spin current accompanies angular momentum, this spin-current emission deprives the magnetization of its angular momentum and thus gives rise to additional magnetization-precession relaxation [12–14]. In the attached metal, in

turn, the spin current injected is converted into an electric current via the SO interaction, a phenomenon called the inverse spin Hall effect (ISHE) [15–23]. This electric current induced by ISHE has recently been observed in a $Ni_{81}Fe_{19}$/Pt film [22].

Now consider the inverse of the above electric current generation: What happens when an electric current is injected in the metal with strong SO interaction attached to
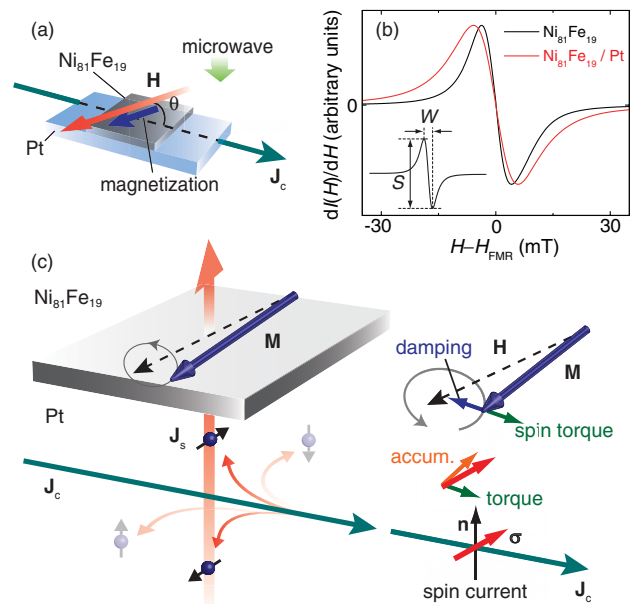

FIG. 1 (color). (a) A schematic illustration of the $Ni_{81}Fe_{19}$/Pt system. **H** and $\mathbf{J}_c$ represent the external magnetic field and the applied electric current, respectively. (b) Field (H) dependence of the FMR signal $dI(H)/dH$ for the $Ni_{81}Fe_{19}$/Pt bilayer film (red) and a $Ni_{81}Fe_{19}$ film (black). Here I denotes the microwave absorption intensity. H_{FMR} represents the ferromagnetic resonance field. The inset shows the definition of spectral width W and spectral intensity S. (c) A schematic illustration of the spin Hall and the spin-torque effects in the present system. **M**, $\mathbf{J}_s$, and $\boldsymbol{\sigma}$ denote the magnetization in the $Ni_{81}Fe_{19}$ layer, the flow direction of the spin current, and the spin-polarization vector of the spin current, respectively.

036601-1

the film magnet? One may expect from the reciprocity that $1/\tau$, namely, the width of the FMR spectra, may be modulated via SHE in the metal, enabling manipulation of the magnetization-precession relaxation of the film in an electric manner. As discussed below, this is actually the fact in a metallic magnet attached to a Pt film, in which this reciprocity affords a clue to our study.

The sample is a simple $Ni_{81}Fe_{19}$/Pt bilayer film comprising a 10-nm-thick ferromagnetic $Ni_{81}Fe_{19}$ layer and a 10-nm-thick paramagnetic Pt layer, as illustrated in Fig. 1(a). The details of the sample preparation are described in Ref. [22]. The surface of the $Ni_{81}Fe_{19}$ layer is of a 0.48 mm^2 rectangular shape. The FMR spectra were measured with applying an electric current $\mathbf{J}_c$ through electrodes attached to both ends of the Pt layer. Pt exhibits a significant SHE [21] and ISHE [21,22]. In this Pt layer, the SHE converts $\mathbf{J}_c$ into a pure spin current $\mathbf{J}_s$, which propagates into the $Ni_{81}Fe_{19}$ layer through the interface. The spin polarization of this spin current is directed along $\mathbf{J}_c \times \mathbf{n}$ [see Fig. 1(c)] [16], where $\mathbf{n}$ represents the normal vector of the interface plane. During the measurement, the microwave mode with a frequency of $f = 9.441$ GHz exists in the cavity, and an external magnetic field $\mathbf{H}$ is applied along the film plane at the angle θ to the direction across the electrodes [see Fig. 1(a)]. Since the magnetocrystalline anisotropy of $Ni_{81}Fe_{19}$ is negligibly small, the magnetization $\mathbf{M}$ in the $Ni_{81}Fe_{19}$ layer is uniformly aligned along the external magnetic field direction. All of the measurements were performed at room temperature.

Figure 2(a) shows the FMR spectra measured at various values of J_c when $\theta = 90°$. Each spectrum is well reproduced by a simple Lorentz function. In Fig. 2(c), we plot spectral width $W^*(J_c) \equiv W(J_c)/W(0)$ and spectral intensity $S^*(J_c) \equiv S(J_c)/S(0)$ obtained from the spectra. Here S is defined as the total amplitude of the resonance shape [see Fig. 1(b)]. By increasing the current intensity, spectral width W increases and amplitude S decreases gradually. Similar behaviors are observed when $\theta = 0$, as shown in Fig. 2(d). These rough spectral features, that is, W increases and S decreases with $|J_c|$, are attributed to joule heating due to the applied electric current; as temperature increases, the fluctuation of magnetization is enhanced, which suppresses S and enhances the magnetization-precession decay or W [24].

The most notable feature of the FMR spectra is found when exploring the current-polarity dependence of the resonance spectra. In the insets in Figs. 2(a) and 2(b), we show magnified views around the peaks of the spectra at $\theta = 90°$ and 0, respectively. At $\theta = 0$, the spectral shapes are little changed by reversing the electric current polarity [compare the solid and dashed curves in Fig. 2(b)], showing that the current-induced spectral change is due entirely to the heating effect when $\theta = 0$. In contrast, surprisingly, the spectral shapes are clearly modulated by reversing the current polarity when the external field direction is perpendicular to the applied electric currents [$\theta = 90°$; see the inset in Fig. 2(a)]. To show this θ dependence more
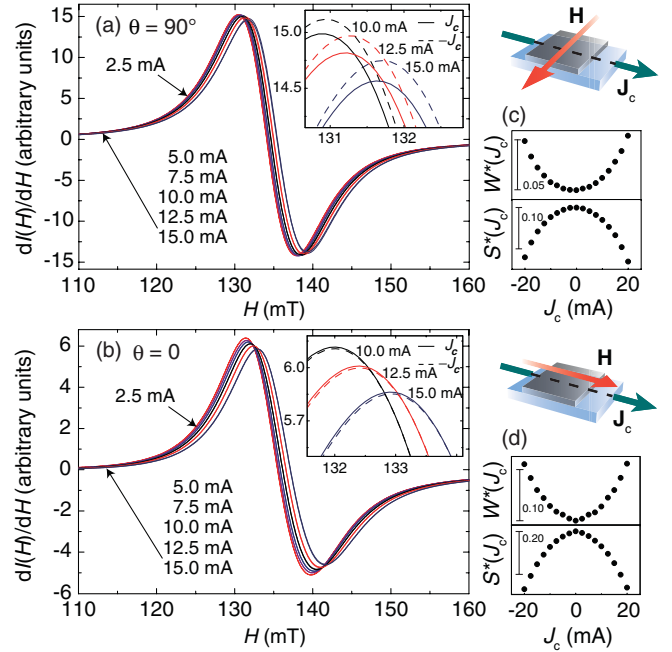

FIG. 2 (color). The FMR spectra for the $Ni_{81}Fe_{19}$/Pt bilayer film measured at various electric current values J_c when the magnetic field direction is (a) $\theta = 90°$ and (b) $\theta = 0$. The inset shows magnified views around the peaks of the spectra, where the solid and dashed curves are the FMR spectra measured with electric currents J_c and $-J_c$, respectively. (c) and (d) show the J_c dependence of the renormalized FMR spectral width $W^*(J_c)$ and intensity $S^*(J_c)$ at $\theta = 90°$ and $\theta = 0$, respectively.

clearly, $dI(J_c)/dH - dI(-J_c)/dH$, obtained from the spectra shown in Figs. 2(a) and 2(b), are plotted in Figs. 3(a) and 3(b), respectively. In contrast to very small signals obtained from $\theta = 0$ data, clear resonance structures in $dI(J_c)/dH - dI(-J_c)/dH$ appear when $\theta = 90°$, demonstrating significant spectral modulation in response to current reversal at $\theta = 90°$.

In order to investigate in detail this unconventional current-induced modulation of the spectral shape, in Fig. 3(c), we plot $\Delta W \equiv W^*(J_c) - W^*(-J_c)$: the asymmetric component of spectral width W^* with respect to J_c. ΔW at $\theta = 0$ is almost zero for all of the J_c values. In contrast, when $\theta = 90°$, ΔW clearly increases with J_c. This indicates that, when $\theta = 90°$, the magnetization relaxation depends on current $\mathbf{J}_c$, besides the heating effect affected by $|\mathbf{J}_c|$. The asymmetric component of the spin relaxation coefficient $\Delta\alpha \equiv \alpha(J_c) - \alpha(-J_c)$ is also plotted in Fig. 3(c), where $\alpha \equiv 1/(2\pi f\tau) = (\sqrt{3}\gamma/4\pi f)W$.

The observed $\mathbf{J}_c$-induced modulation of the relaxation cannot be attributed to magnetic field effects induced by the electric current. Figure 3(d) shows ΔW observed for a $Ni_{81}Fe_{19}$/Cu film, a similar system in which the Pt layer is replaced by Cu, and a plain $Ni_{81}Fe_{19}$ film in which the Pt layer is missing, at $\theta = 90°$. ΔW for the plain $Ni_{81}Fe_{19}$ film shows no $\mathbf{J}_c$ dependence even when an electric current is applied in the film, indicating that a possible small flow of electric currents in the $Ni_{81}Fe_{19}$ layer in the $Ni_{81}Fe_{19}$/Pt
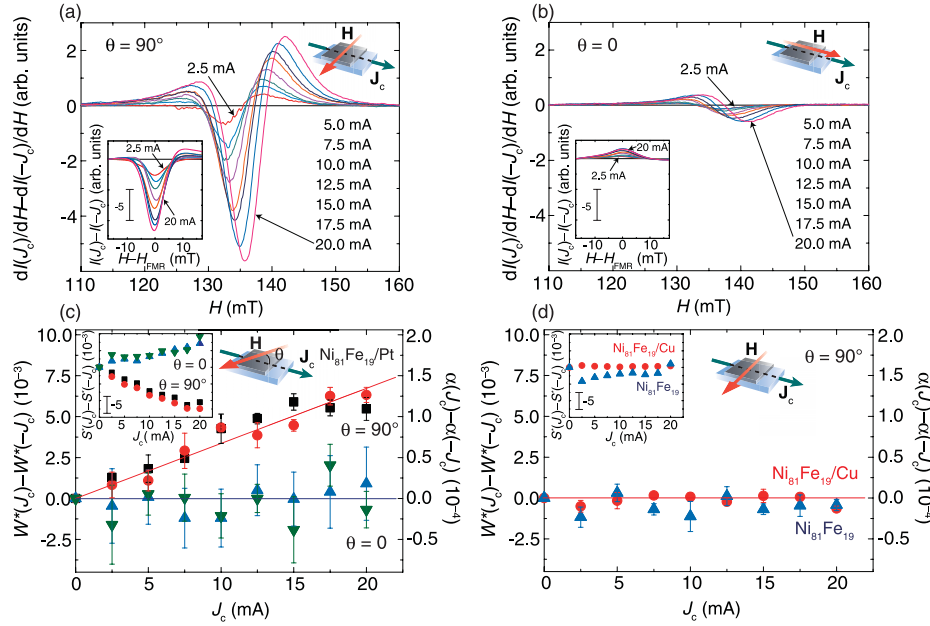
FIG. 3 (color). (a),(b) The $dI(J_c)/dH - dI(-J_c)/dH$ spectra for the $Ni_{81}Fe_{19}/Pt$ film at $\theta = 90°$ and 0 for various J_c values, respectively. The inset shows the H dependence of $I(J_c) - I(-J_c)$. (c) The J_c dependence of $\Delta W \equiv W^*(J_c) - W^*(-J_c)$ for the $Ni_{81}Fe_{19}/Pt$ bilayer film at $\theta = 90°$ (black and red) and 0 (blue and green). Here $W^*(J_c) \equiv W(J_c)/W(0)$. The J_c dependence of $\Delta\alpha \equiv \alpha(J_c) - \alpha(-J_c)$ is also plotted. The inset shows $\Delta S \equiv S^*(J_c) - S^*(-J_c)$. The data in different colors, namely, the red (blue) and the black (green) data, were measured in different samples. The lines in red and blue are linear fits to the data at $\theta = 90°$ and $\Delta\alpha = 0$, respectively. (d) ΔW measured for a $Ni_{81}Fe_{19}/Cu$ bilayer film (red) and a $Ni_{81}Fe_{19}$ film (blue) at $\theta = 90°$. The inset shows ΔS. The red line represents $\Delta\alpha = 0$.

system is irrelevant to the observed relaxation modulation shown in Fig. 3(c). ΔW for the $Ni_{81}Fe_{19}/Cu$ film also shows no $\mathbf{J}_c$ dependence when applying an electric current through the electrodes attached to the Cu layer. This demonstrates that the observed $\mathbf{J}_c$-induced modulation of the spectral width in the $Ni_{81}Fe_{19}/Pt$ system cannot be attributed to the inhomogeneity of the magnetic field (Oersted field) induced by the electric current. In fact, the averaged value of the Oersted field induced at the $Ni_{81}Fe_{19}$ layer of the $Ni_{81}Fe_{19}/Pt$ system by the current $J_c = 20$ mA is estimated from the resonance-field variation to be 0.039 mT, a value much smaller than the resonance field 135 mT and smaller than the shift of the spectral valley in Fig. 3(a) (3 mT). The latter represents the magnetization reduction due to the current-induced joule heating. The thermoelectric effects are also irrelevant; we monitored temperature at the surface of the $Ni_{81}Fe_{19}$ layer using a microthermocouple, and the temperature was found not to be affected by the current reversal.

The observed unconventional modulation of the relaxation is best interpreted in terms of the macroscopic spin transfer induced by the strong SHE [21,22] in the Pt layer. Notable is that, when $\theta = 90°$, at which $\mathbf{J}_c$-induced FMR modulation is observed, the external magnetic field is directed along the spin-polarization direction of the spin current generated $\mathbf{J}_c \times \mathbf{n}$ [see Fig. 1(c)]. This spin current is injected into the whole $Ni_{81}Fe_{19}$ layer owing to the SHE. In this situation, the spin torque acting on the $Ni_{81}Fe_{19}$

layer draws the magnetization toward ($J_c > 0$) or away from ($J_c < 0$) the external magnetic field direction. Since this torque is parallel or antiparallel to the Gilbert-damping torque, it modulates the relaxation of the magnetization precession in the whole $Ni_{81}Fe_{19}$ layer.

We develop a model for the precessing magnetization in a F($Ni_{81}Fe_{19}$)/N(Pt) film and calculate the modulation of the relaxation coefficient due to the SHE in the Pt layer. The dynamics of the magnetization in the F layer can be described by a generalized Landau-Lifshitz-Gilbert (LLG) equation [5] with the torque terms due to the spin pumping [13] and the SHE. At $J_c = 0$, only the spin pumping contributes to the relaxation of the precessional motion, and yields an additional Gilbert-damping constant $\Delta\alpha_{SP}$ to the intrinsic damping constant α_F of an isolated F layer [13,14], the sum of which is denoted as $\alpha_0 = \alpha_F + \Delta\alpha_{SP}$ and independent of J_c. At $J_c \neq 0$, the SHE contributes to further relaxation, since the transverse component of the injected spin current generated by SHE is transferred to the magnetization, exerting the spin-transferred torque on $\mathbf{M}$. Thus, the generalized LLG reads $d\mathbf{M}/dt = -\gamma\mathbf{M} \times \mathbf{H}_{eff} + (\alpha_0/M_s)\mathbf{M} \times d\mathbf{M}/dt - (\gamma J_s^{SHE}/M_s^2 V_F)\mathbf{M} \times (\mathbf{M} \times \boldsymbol{\sigma})$, where the effective field $\mathbf{H}_{eff} = \mathbf{H} - 4\pi M_x\hat{\mathbf{x}} + \mathbf{h}_{ac}$ is the sum of the in-plane applied field $\mathbf{H}$, the demagnetizing field $-4\pi M_x\hat{\mathbf{x}}$, and the microwave field $\mathbf{h}_{ac} = (0, h_{ac}e^{-2\pi ift}, 0)$, with microwave frequency f. J_s^{SHE} is the spin current injected into the F layer, M_s is the saturation magnetization of the F layer, and V_F is the

volume of the F layer. For the setup in Fig. 2(a) ($\theta = 90°$), in which $\boldsymbol{\sigma}$ is parallel to the precession axis $\hat{\mathbf{z}}$, the linearized LLG equation with respect to the precession amplitude is solved to yield analytical expressions for $\mathbf{M}$, from which we can calculate the total relaxation coefficient $\alpha = \alpha_0 + \Delta\alpha_{\mathrm{SHE}}$, where $\Delta\alpha_{\mathrm{SHE}}$ due to SHE is given by

$$\Delta\alpha_{\mathrm{SHE}} = \frac{(\gamma J_s^{\mathrm{SHE}}/2\pi f M_s V_{\mathrm{F}})}{\sqrt{1 + (\frac{\gamma M_s}{f})^2 - (\frac{\gamma J_s^{\mathrm{SHE}}}{2\pi f M_s V_{\mathrm{F}}})^2}} \approx \frac{\gamma J_s^{\mathrm{SHE}}}{2\pi f M_s V_{\mathrm{F}}}. \quad (1)$$

Here $\gamma M_s/f \approx 1$ and $\gamma|J_s^{\mathrm{SHE}}|/(2\pi f M_s V_{\mathrm{F}}) \ll 1$ are used. In the Pt layer, the applied current J_c generates the spin Hall current $\theta_{\mathrm{SHE}}\hat{\mathbf{z}} \times \mathbf{J}_c$. Incorporating the spin Hall current in the drift-diffusion equation [25–27] and solving them in the bilayer film with the transparent interface approximation, we obtain the injected spin current $J_s^{\mathrm{SHE}} = \eta\theta_{\mathrm{SHE}}A_{\mathrm{F/N}}(\hbar/e)(J_c/A_{\mathrm{N}})$, where $A_{\mathrm{F/N}}$ is the area of the interface, A_{N} is the cross-sectional area of the N layer, and η is the injection efficiency $\eta = 2\sinh^2(d_{\mathrm{N}}/2\lambda_{\mathrm{N}})/\cosh(d_{\mathrm{N}}/\lambda_{\mathrm{N}})/[1 + (\lambda_{\mathrm{F}}/\lambda_{\mathrm{N}})(\sigma_c^{\mathrm{N}}/\sigma_c^{\mathrm{F}}) \times \tanh(d_{\mathrm{N}}/\lambda_{\mathrm{N}})/\tanh(d_{\mathrm{F}}/\lambda_{\mathrm{F}})]$, with the thickness d_{N} (d_{F}), the electrical conductivity σ_c^{N} (σ_c^{F}), and the spin diffusion length λ_{N} (λ_{F}) of the N (F) layer. Thus, Eq. (1) becomes

$$\Delta\alpha_{\mathrm{SHE}} \approx \left(\frac{\hbar\gamma\eta\theta_{\mathrm{SHE}}}{2\pi f M_s e A_{\mathrm{N}} d_{\mathrm{F}}}\right)J_c, \quad (2)$$

indicating that the damping varies linearly with J_c. The asymmetric component of the relaxation coefficient is given by $\Delta\alpha = 2\Delta\alpha_{\mathrm{SHE}}$ owing to the cancellation of α_0, and therefore $\Delta\alpha_{\mathrm{SHE}}$ is directly related to the W modulation. When $\theta = 0$, $\Delta\alpha_{\mathrm{SHE}}$ vanishes because the spin torque due to the SHE is canceled out during the precession motion. These J_c-dependent features are consistent with the experimental results shown in Fig. 3. The calculated W modulation, i.e., $W(J_c) - W(-J_c) = (4\pi f/\sqrt{3}\gamma)2\Delta\alpha_{\mathrm{SHE}}$, is proportional to the amplitude of the spin current injected into the F layer, and the spin-current amplitude is measured by monitoring W; this modulation can thus be used as a spin-current meter.

At $J_c = 0$, spectral width W and relaxation coefficient α were estimated to be $W(0) = 7.39$ mT and $\alpha(0) = 0.02$, respectively. The red line in Fig. 3(c) is a fit to the data for $\theta = 90°$, which yields $\eta\theta_{\mathrm{SHE}} \sim 0.03$ for $4\pi M_s = 610$ mT and $f = 9.441$ GHz. For parameters of $\sigma_c^{\mathrm{Pt}} = 0.064$ $(\mu\Omega\,\mathrm{cm})^{-1}$, $\sigma_c^{\mathrm{Py}} = 0.065$ $(\mu\Omega\,\mathrm{cm})^{-1}$, $\lambda_{\mathrm{Pt}} = 7$ nm, $\lambda_{\mathrm{Py}} = 3$ nm at room temperature [21,28], and $d_{\mathrm{Pt}} = d_{\mathrm{Py}} = 10$ nm, the injection efficiency is $\eta \sim 0.4$, and hence the spin Hall angle of the Pt layer is $\theta_{\mathrm{SHE}} \sim 0.08$, which is comparable to the value 0.113 reported by Seki *et al.* [29] but much larger than the value 0.0037 reported by Kimura *et al.* [21], the difference of which might be attributed to impurity species and left to be elucidated in further studies. From the experimental data and Eq. (1), the spin torque acting on the $\mathrm{Ni}_{81}\mathrm{Fe}_{19}$ layer,

$2\pi f M_s V_{\mathrm{F}}\Delta\alpha_{\mathrm{SHE}}/\gamma$, induced by the SHE in the present system is estimated to be 4.7×10^{-14} J at 20 mA.

* kazuya_ando@z8.keio.jp

[1] S. Chikazumi, *Physics of Ferromagnetism* (Oxford University, Oxford, 1997), 2nd ed.
[2] S. A. Wolf *et al.*, Science **294**, 1488 (2001).
[3] I. Zutic, J. Fabian, and S. Das Sarma, Rev. Mod. Phys. **76**, 323 (2004).
[4] B. E. Kane, Nature (London) **393**, 133 (1998).
[5] J. C. Slonczewski, J. Magn. Magn. Mater. **159**, L1 (1996).
[6] J. Grollier *et al.*, Appl. Phys. Lett. **78**, 3663 (2001).
[7] S. I. Kiselev *et al.*, Nature (London) **425**, 380 (2003).
[8] A. A. Tulapurkar *et al.*, Nature (London) **438**, 339 (2005).
[9] J. C. Sankey *et al.*, Phys. Rev. Lett. **96**, 227601 (2006).
[10] Yisong Zhang *et al.*, J. Appl. Phys. **101**, 103905 (2007).
[11] A. H. Morrish, *The Physical Principles of Magnetism* (Robert E. Krieger, New York, 1980), p. 568.
[12] R. H. Silsbee, A. Janossy, and P. Monod, Phys. Rev. B **19**, 4382 (1979).
[13] Y. Tserkovnyak, A. Brataas, and G. E. W. Bauer, Phys. Rev. Lett. **88**, 117601 (2002).
[14] S. Mizukami, Y. Ando, and T. Miyazaki, Phys. Rev. B **66**, 104413 (2002).
[15] M. I. Dyakonov and V. I. Perel, Phys. Lett. **35A**, 459 (1971).
[16] J. E. Hirsch, Phys. Rev. Lett. **83**, 1834 (1999).
[17] S. Murakami, N. Nagaosa, and S. C. Zhang, Science **301**, 1348 (2003).
[18] J. Sinova *et al.*, Phys. Rev. Lett. **92**, 126603 (2004).
[19] Y. K. Kato, R. C. Myers, A. C. Gossard, and D. D. Awschalom, Science **306**, 1910 (2004).
[20] J. Wunderlich, B. Kaestner, J. Sinova, and T. Jungwirth, Phys. Rev. Lett. **94**, 047204 (2005).
[21] T. Kimura, Y. Otani, T. Sato, S. Takahashi, and S. Maekawa, Phys. Rev. Lett. **98**, 156601 (2007).
[22] E. Saitoh, M. Ueda, H. Miyajima, and G. Tatara, Appl. Phys. Lett. **88**, 182509 (2006).
[23] S. O. Valenzuela and M. Tinkham, Nature (London) **442**, 176 (2006).
[24] S. M. Bhagat and E. P. Chicklis, Phys. Rev. **178**, 828 (1969).
[25] T. Valet and A. Fert, Phys. Rev. B **48**, 7099 (1993).
[26] S. Takahashi, H. Imamura, and S. Maekawa, in *Concepts in Spin Electronics*, edited by S. Maekawa (Oxford University, Oxford, 2006).
[27] S. Takahashi and S. Maekawa, Phys. Rev. Lett. **88**, 116601 (2002); J. Magn. Magn. Mater. **310**, 2067 (2007).
[28] J. Bass and W. P. Pratt, Jr., J. Phys. Condens. Matter **19**, 183201 (2007).
[29] T. Seki *et al.*, Nat. Mater. **7**, 125 (2008).